MEMS WITH AN EMBEDDED FLUIDIC MICROCHANNEL FOR SENSITIVE WEIGHING OF LIQUID SAMPLES

Céline Hadji[1], Léopold Virot[1], Cyril Picard[2], François Baléras[1], and Vincent Agache[1]
[1]CEA/LETI, FRANCE
[2] University Grenoble Alpes, Liphy, FRANCE

ABSTRACT

This paper reports hollow MEMS plate oscillators for the characterization of liquid samples, with a one-fold improvement in both Q-factor and Allan deviation compared to previous alike structures, and fluidic constriction larger than 1µm. These new characteristics make the devices amenable for the first time to liquid weighing with a 100 Hz.(g.L^{-1})$^{-1}$ sensitivity and a few g.L^{-1} detection floor.

INTRODUCTION

The development of MEMS/NEMS mass sensors has boomed considerably in the last 2 decades. As an illustration, Ref [1] offers a consistent review of the existing techniques based on MEMS sensors for liquid samples characterization. Generally, the optimization of these sensors requires the resonator to be light and to ring with a relatively high quality factor. However, this strategy is impeded when it requires the immersion of the sensor in the fluid, especially because of damping of the vibration by the compression of the viscous fluid.

One of the most promising approaches is addressing this constraint by enclosing a micro- nanofluidic channel in a MEMS resonator, eliminating drastically the viscous damping with the liquid. This concept has been initially introduced by E. Stemme *et al.* for liquid density measurement (density sensitivities of the order of -200 ppm/(kg m^{-3}) with silicon tube vibrating in torsional mode [2]. Recently, it was adapted by Scott Manalis group at MIT [3] and further optimized in terms of design to enable precise measurements of growth kinetics of single cells, assessment of cellular responses to drugs [4] and even weigh individual nanoparticles [5]. This concept, named suspended microchannel resonator (SMR), consists of a micromechanical cantilever with a microfluidic channel confined into the core of the resonator while the SMR vibrates in a dry medium (vacuum packaged cavity).

In this work, this principle has been extended by applying it to hollow thin plates (called plates SMR hereinafter), enabling operation at atmospheric pressure with quality factor of a few thousands. Incidentally these structures and the in-plane mode are more suited to co-integrated transduction, prerequisite for large-scale integration.

DESIGNS

The Fig. 1 illustrates the design of typical sensors, consisting of plate SMR with a square geometry, alternatively a disk shaped geometry, suspended above a cavity by four beams, each being located at a vibration node for the studied mode. The square, and disk plates are designed to operate according to the lamé or wine-glass, mode respectively. The structure mechanical vibrations are characterised by the entire plate contracting and extending in the plane of motion as shown on Fig 1c. The resonators vibration is produced thanks to a lateral electrostatic coupling with facing electrodes across a transduction gap, scaled down to 1µm. As the structure is brought into vibration, the capacitance across the sense electrodes is modulated due to changes in the gap, which in turn produces a motional current I_m whose amplitude is maximum at the resonance frequency of the device.

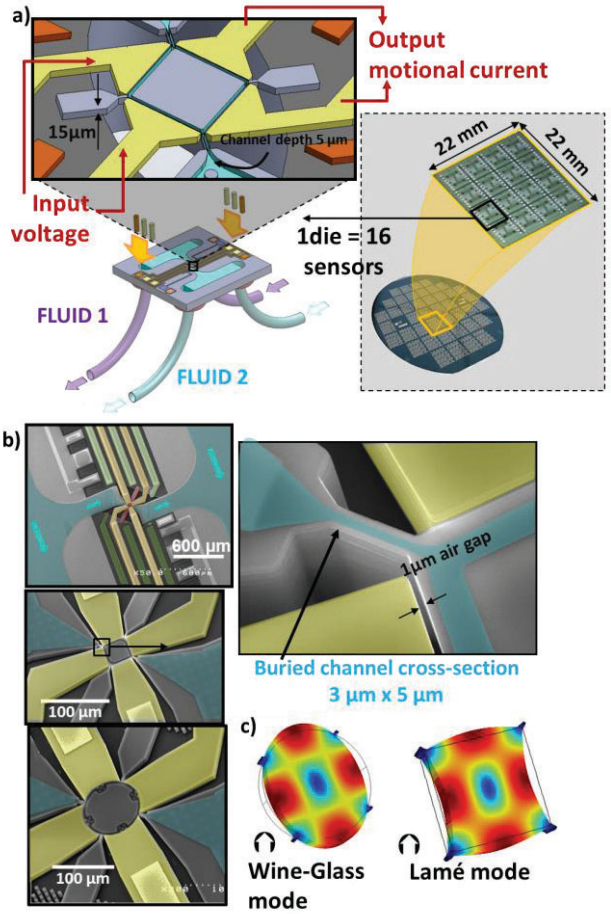

Figure 1: a) Schematic of a die, including 16 independent sensors (hollow plates). b) SEM colored pictures of a 50µm-wide square plate and a 100µm-wide disk plate. c) Lamé and Wine-glass mode shape of a square and a disk plate respectively, simulated with COMSOL Multiphysics®.

In contrast to previous generation of alike plate-type SMRs developed by the authors [6], the sensors in this work differ by specific improvements to allow faster operation and better sensitivity, as detailed in the following.

- The buried channel is now etched along the plate edges. Thus, better mass responsivity is expected

since channel location is matching areas of maximum amplitude of vibration.

- The buried channel in the SMR is now in a bypass configuration between upstream and downstream channels to enable faster filling fluidic procedure and increase the analysis throughput. This bypass channel network is supplied with fluids across 4 inlet and outlet ports etched through the backside silicon substrate.
- The constraints of wire bonding and capillaries gluing have been eliminated for these devices, by physically decoupling the fluidic supply (performed at the backside) and electrical connections (front side of the device). With this strategy, the die is interfaced through a customized plug and play platform.

The square and disk plate SMR devices which have been experimentally tested in this study were 150µm and 200 wide, resulting in a fundamental resonant frequency ranging from 20 to 20.6MHz.

SETUP

« Plug and play » test platform

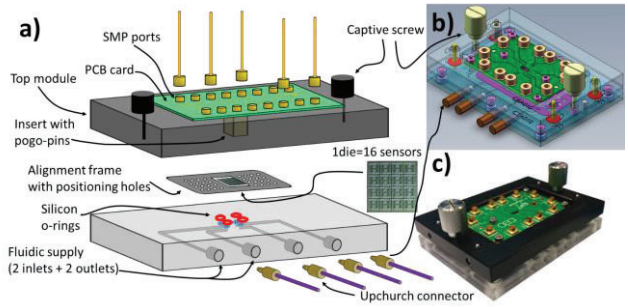

Figure 2: (a) Exploded view drawing of the platform, including the top piece for electrical connection, bottom piece for fluidic delivery and the intermediate alignment frame. (b) CAD three-dimensional diagram of the platform. (c) Optical photography of the platform with transparent PMMA lower piece.

A plug and play connection platform, as illustrated on Figure 2, was designed and manufactured in order to allow for fast and easy electrical and fluidic interfacing with the sensors. The concept is based on two pieces and an intermediate frame for positioning the die:

- A top piece is holding a Printed Circuit Board (PCB) with SMP connectors arranged in the periphery and pogo pins housed in an insert located in the center of the PCB. The center distance between each pogo-pin corresponds to the distance between two adjacent electrical contacts patterned on the chip.
- A bottom transparent card made of PMMA includes 4 microscale fluidic channels to deliver the fluid from pressurized vials connected to a Flow Control System (from Fluigent MFCS-EZ) toward the chip. Silicone o-rings are inserted around protruding hollow stems on the card front side to ensure a fluid tight connection to the chip fluidic inlet/outlet ports without leakage.
- An intermediate alignment frame, made of stainless steel, and having micromachined slots, positioned complementarily with respect to the cleavage bridges located on the edge of each die. When the die is inserted into the frame, its outline follows the notched inner edge of the frame so that the pogo-pins and silicone o-rings inserted in the bottom piece are self-aligned with respectively the electrical contact pads and fluidic access holes arranged on the chip. Furthermore, the alignment frame features on its periphery two arrays of drilled patterns (16x2 circular holes in this case). Depending on the sensor to be tested on the die (which has 16 independent sensors), a pair of 2 holes (one per network) will be selected so as to insert into each a positioning pin fixed to the bottom piece.

Electrical setup

Similarly to the Ref [7], the resonators are tested using fully differential setup (shown on Fig. 3) to reduce the capacitive feedthrough between driving and sensing electrodes. The differential setup is slightly modified in the sense that the DC voltage which adjusts the transduction efficiency, is applied to the four lateral electrodes, isolated from the AC signal by a bias tee, whereas the resonator is grounded. The aim of this configuration is to avoid any electrolysis which may occur when flowing ionic solutions in the sensor buried channel.

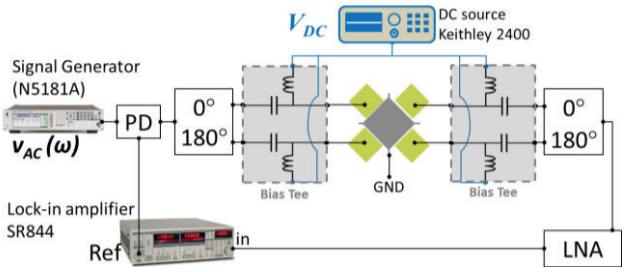

Figure 3: Diagram of the electrical setup for the sensors characterization. The experimental setup includes a DC voltage source, a low noise amplifier (LNA), a frequency synthesizer, a power divider (PD) splitting the ac signal to a 180° power splitter for driving the sensor, and to a lock-in amplifier (Stanford Research Systems) for supplying a reference signal.

Fluidic setup

The microchannel network inside the die is H-shaped and the buried channel in the resonator is in bypass configuration between the two lateral microscale channels. By adjusting the pressure gradient between the upstream and downstream microscale channels, it is possible to control accurately the flow rate inside the buried channel, and quickly exchange the solutions to be injected into the resonator. Towards this purpose, fluids are delivered to the device inlet/outlet ports using pressurized vials connected to a microfluidic Flow Control System from Fluigent (MFCS-EZ). Liquid flow meters from Sensirion (SLG1430-150) are connected in series in the lateral channels in order to monitor in real time flows and to estimate the flow rate inside the bypass channel through the buried resonator. Inline-filters (1µm and 2µm porosity) are also included to provide protection of the chip regarding larger particles clogging. The setup includes a 4-ways valve to allow exchange of solutions to be inserted into the chip without disconnecting and draining it. The Fig. 4 illustrates the schematic image of the setup, as well as labels for definition of hydraulic

resistances in each branch, pressures and flow rates. Pressures Pe and Ps are applied respectively on the two inlet vials (P1 = P2 = Pe), and both outlet vials (P3 = P4 = Ps). Because of different capillary lengths (50cm long in case of track 3, and 35cm long in case of track 4) connecting the chip outlets, a pressure gradient and flow rate through the buried channel is then induced.

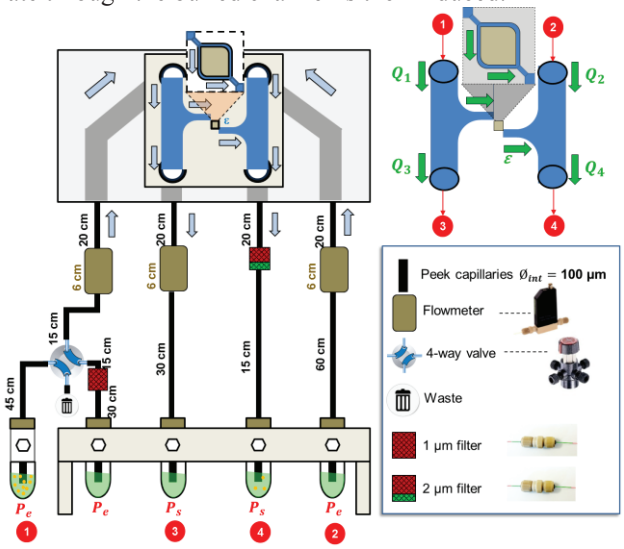

Figure 4: schematic image of fluidic setup. Pressurized vials are connected to the chip inlet and outlet ports (1 to 4) and flowmeters to monitor the flow inside of the chip.

EXPERIMENTS

Tests without fluid

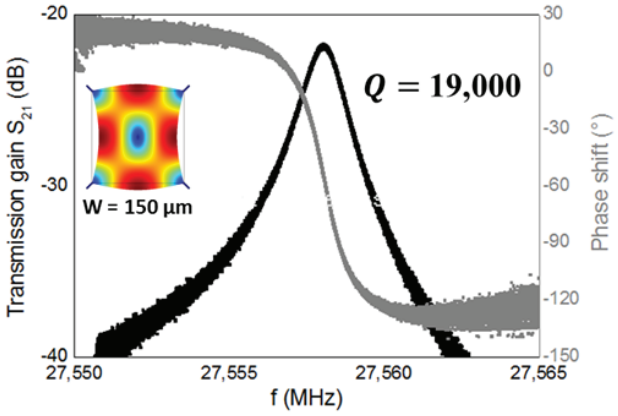

Figure 5: Transmission curves (amplitude and phase) for a 150 µm-wide square plate sensor.

In following experiments, the lock-in time constant was set at 30ms. Fig 5 shows typical electrical transmission (both magnitude and phase curves superimposed) for a 150µm wide square-plate SMR in air, wherein a DC bias voltage of 80V and driving ac signal of 1.26 Vrms were applied to the drive electrodes according to the setup shown in Fig 3. A quality factor of 19,000 is extracted at the resonance by measuring the width of the transmission peak at -3dB.

Mass resolution for the sensors can be estimated by running Allan deviation analysis which gives the frequency stability of the device, including the electrical setup noise sources. Allan deviation computation was carried out in closed loop configuration using the PLL developed in Ref.[8]. Typical analysis is shown on fig 6 with corresponding mass resolution δM, determined as $\delta M \approx 2 m_{EFF} \cdot \sigma(\tau_e)$, with m_{EFF} the oscillator effective mass and τ_e the integration time. In example given here, mass resolution is in the order of the fg for ms integration time.

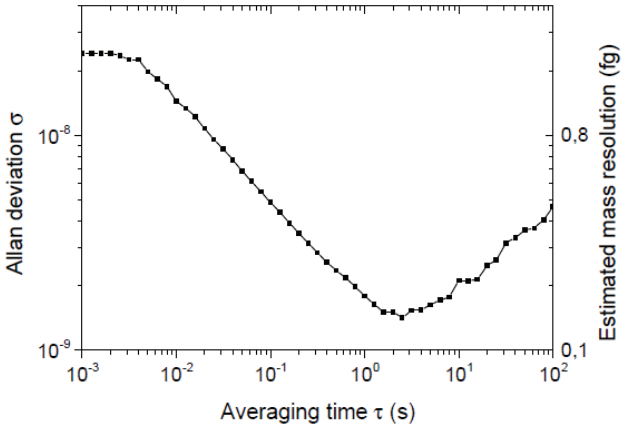

Figure 6: Calculated Allan deviation and corresponding mass resolution for a 150µm-wide square plate SMR with an empty channel.

Tests with fluid

First the expression of the resonant frequency of a SMR resonator is recalled as a function of the added mass of fluid inserted into the buried channel:

$$f_{0_{fluid}} = \frac{1}{2\pi}\sqrt{\frac{k_{eff}}{m_{eff} + \alpha\, m_{fluid}}} \qquad (1)$$

where α is an impact factor of the added mass on the resonant frequency. For flexural cantilevers-type SMRs, α takes on a value of 0.24 for changes in solution density [3]. In the following, the impact on the plate SMR sensors response of the fluid density and viscosity is evaluated. Aqueous samples with different concentrations were prepared, degassed and filtered. Trisodium citrate, NaCl and BaCl2-water mixings samples were used to evaluate the mass sensitivity of our devices (no impact of the viscosity is assumed given the concentration of the solutate). Glycerol-water-ethanol mixings were prepared to study the influence of the viscosity on the sensor's response.

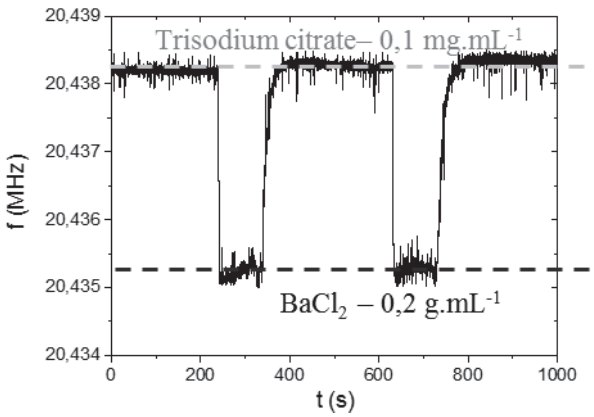

Figure 7: Resonance frequency observed during a PLL measurement when two fluids of different density are injected alternately into a 200µm wide square plate SMR.

The injection of the different fluids is achieved by changing the position of the valve included in the setup. It is also possible to alternate the weighing of two different solutions previously inserted in the upstream and

downstream lateral channels, by modifying the pressures applied to the terminals of the buried channel. Fig. 7 shows two plateau in the frequency measurement of a 200µm wide square plate SMR alternating the filling of buried channel with dissolved trisodium citrate (concentration of 0.1 mg.mL^{-1}) and BaCl2 (concentration of 0.2 g.mL-1), while operating the device in a PLL configuration. From the data in Fig. 7, an impact coefficient of 0.72 is evaluated, which potentially reveals a better mass sensitivity for such device as compared to cantilever type SMRs.

To go further, a 200µm-wide disk plate was used in the following to weigh solutions with various compositions, densities and viscosities. A series of experiments was conducted to extract the sensor's sensitivity, by flowing NaCl, BaCl2, and Glycerol solutions (with various concentration and corresponding mass density), and measuring the resulting frequency shift, each point being the average of 3 to 6 values.

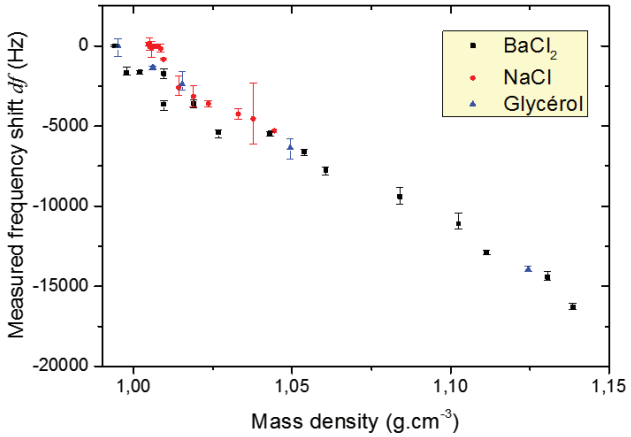

Figure 8: Frequency shift as a function of the mass density of NaCl, BaCl2, Glycerol solutions injected into a 200µm wide disk plate SMR.

A sensitivity of 100 kHz (g.cm^{-3})$^{-1}$ was inferred by linear regression applied to the measurements with $BaCl_2$ solutions (*ie* our most "complete" measurements). This is 10 folds improvement as compared to the sensitivity of cantilever type SMRs. In case of $BaCl_2$ solutions, an average error of 300 Hz is extracted, corresponding to an accuracy of about 3.10^{-3} g.cm^{-3} on the measurement. As a comparison, the DMA500 densimeter commercialized by Anton Paar® has a 10^{-3} g.mL^{-1} accuracy but requires at least 1mL samples, when our sensor needs only a few µL, which is more adapted for expensive reagents. Lastly an impact factor of ~0.4 is deduced, which is smaller as compared to square plate devices (likely due to a lower correction factor in the effective mass calculation).

Lastly, Glycerol-water mixings were used to study the impact of the viscosity on the sensor's response. 3 solutions with different volume ratios of water, glycerol and ethanol were prepared. While having similar mass density (around 1.1g.cm^{-3}), their viscosity varies from 1.1x10^{-2} Pa.s to 7.7x10^{-2} Pa.s. As one can notice on Fig. 8, linear approximation upon mass density remains valid, with a sensitivity of 105 kHz (g.cm^{-3})$^{-1}$. Interestingly the frequency shifts respectively measured for solutions 3 and 4 are of the same order of magnitude despite the factor of 2 between their viscosities. We suspect that the impact of liquid viscosity to the sensor response is limited because of the 2% volume ratio of the liquid channel over the plate, when SMR cantilevers have a typical ratio larger than 20% [3].

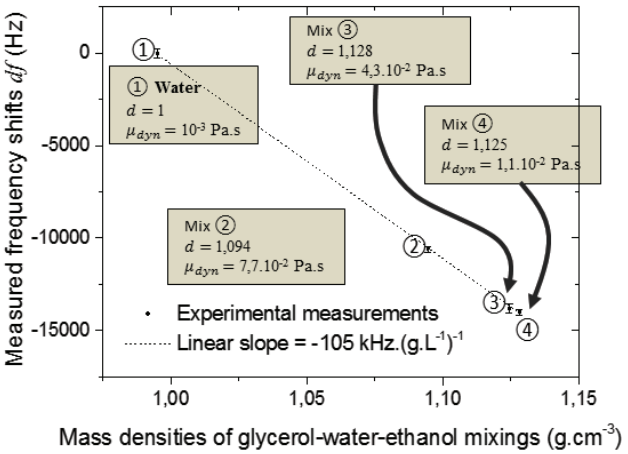

Figure 9: Frequency shift as a function of the mass density of water and Glycerol-water-ethanol mixing solutions injected into a 200µm wide disk plate SMR.

CONCLUSION

Plate SMR sensors for mass density characterization of liquid samples have been presented. Solutions of various density, viscosity and compositions have been weighted, resulting in a sensitivity of the devices of 100-110 kHz.(g.cm^{-3})$^{-1}$, an accuracy in the range of 10^{-3} g.mL^{-1}, which is as good as commercialized densimeters (which typically require larger amounts of solutions, not adapted for expensive reagents), and no appreciable dependence over the fluid viscosity (in the range of 10^{-3} to 8x10^{-2} Pa.s).

ACKNOWLEDGEMENTS

The authors would like to thank Martine Cochet for its valuable help during the dies fabrication process in the clean-room, and Claude Chabrol who contributed to the designing of the connection platform.

REFERENCES

[1] J. Tamayo *et al.*, Chem. Soc. Rev., vol. 42, no. 3, pp. 1287–311, Feb. 2013.
[2] P. Enoksson, et al., Sensors and Actuators A, Vol. 47(1-3), p. 327-331, 1995.
[3] T.P. Burg, et al., Nature 446, 1066-1069, (2007).
[4] N Cermak, et al., Nature Biotechnology, 34, pp. 1052–1059, 2016
[5] S. Olcum et al., PNAS, Jan 12, 2014.
[6] G. Blanco-Gomez and V. Agache, IEEE JMEMS, vol. 21, no. 1, pp. 224–234, Feb. 2012
[7] S.A. Bhave, et al, Proc. IEEE MEMS 2005 (Miami), pp 223–226, 2005.
[8] G. Blanco-Gomez, Eet al., IEEE Electron Device Letters, Vol. 33, No. 4, pp. 609-611, April 2012

CONTACT

*V. Agache, vincent.agache@cea.fr